

Study of residual stresses in electron beam welded constructive steel *via* neutron diffraction method

D. Kaisheva^{1*}, P. Petrov¹, G. Bokuchava², I. Papushkin²

¹ Institute of Electronics, Bulgarian Academy of Sciences, 72 Tzarigradsko Chaussee, 1784 Sofia, Bulgaria

² Frank Laboratory of Neutron Physics, Joint Institute for Nuclear Research, 6 Joliot-Curie str., 141980 Dubna, Russia

Received August 11, 2019; Accepted November 31, 2019

In this work a non-destructive neutron diffraction method was used to determine the residual stress distributions in the gear wheel car transmission manufactured from alloyed steel and welded by electron beam. The residual stress in electron beam welded plates from the same steel was investigated. Time-of-flight neutron diffraction experiments were performed on an FSD diffractometer at an IBR-2 fast pulsed reactor at JINR (Dubna, Russia). The neutron diffraction method allowed evaluating the stress distribution in the radial and axial components of the shaft gear with welded disk. It was found that the residual stress level is quite low in the welding joint. The maximal stress level is varying in the range from 300 MPa to 800 MPa for welded plates and it is up to 500 MPa for the gear wheel. The structure of the material in the welded seam and the heat-affected zone was also examined.

Keywords: Electron beam welding, Residual stress, Neutron diffraction

INTRODUCTION

Steel is an extremely widespread material in the industry and everyday life. There are a large number of varieties of steel, distinguished by the alloying elements and by their properties [1]. The steel that we study, 12XH3A, is low alloyed steel, which is used for the production of gears, shafts, piston pins and other elements. The requirements for such elements include high strength, plasticity and strength of the core and high hardness of the surface as these parts work under heavy impact loads or at low temperatures (up to -100 °C). This type of steel is also used to produce hot-rolled steel plates, bimetal seamless pipes for shipbuilding with an outer layer of steel and an inner layer of copper.

The electron beam welding (EBW) as a method of joining of two metal parts is characterized by a narrow and deep weld, a small heat-affected zone (HAZ) and a lack of impurities of other materials in the seam [2]. As with any other type of welding, residual stresses and deformations occur during EBW as well. Their measurement can be done by applying destructive and non-destructive methods [3]. Among these methods is the method of neutron diffraction. It is non-destructive, allows large-depth measurement due to the high penetration depth of neutrons, high precision, high resolution. Furthermore, this method allows the measurement of macrostress and microstress.

In this work we present the results of the measurement of the residual stresses in EBW of a real gear wheel for a gearbox of a sports car and in two EBW specimens of the same material prepared

of two plates under different technological parameters. A theoretical model for determining the temperature distribution is presented. The structure of the recrystallized material was examined.

METHOD OF MEASUREMENT AND MODELING

Neutron diffraction method

The residual stresses in welding are caused by the microstrains which result from the crystallization of the molten material under the conditions of large temperature gradients. These microstrains find expression in the change of the crystal lattice constant [4]. As a result of this change a displacement of the diffraction spectrum maxima for the deformed lattice is observed, in contrast to the non-deformed one.

The principle of determining the crystal lattice strain *via* the neutron diffraction method is based on the condition of diffraction maximum according to Bragg's law:

$$n\lambda = 2d_{hkl}\sin\theta \quad (1)$$

where λ is the neutron wavelength, d_{hkl} is the interplanar spacing, and θ is the Bragg angle or the angle of incidence and scattered rays, n is an integer.

Depending on the neutron wavelength, the peak position on the time scale is defined by the condition:

$$t = \frac{L}{v} = \frac{\lambda mL}{h} = \frac{2mLd_{hkl}\sin\theta}{h} \quad (2)$$

where L is the total flight distance from a neutron source to the detector, v is the neutron velocity,

* To whom all correspondence should be sent.

E-mail: darinakaisheva@abv.bg

In a neutron pulse flow, a difference in time-of-flight (TOF) of neutrons is observed. Hence, in the case of TOF neutron diffraction the lattice strain is determined as:

$$\varepsilon_{hkl} = \frac{d_{hkl} - d_{hkl}^0}{d_{hkl}^0} = \frac{\Delta t}{t} \quad (3)$$

where d_{hkl} and d_{hkl}^0 are the interplanar spacings for strained and unstrained lattices.

Heat model

The model gives a possibility for calculating the temperature field during welding. It is based on a solution of the classical heat conduction equation:

$$\rho c_p \frac{\partial T}{\partial t} + \nabla(-\lambda \nabla T) = f(r, t) \quad (4)$$

where c_p is specific heat, ρ is density and λ is thermal conductivity of the material and the heat distribution of the beam corresponds to the heat source $f(r, t)$.

In case that c_p , ρ and λ are not dependent on the temperature and $\alpha = \lambda/\rho c_p$ is the thermal diffusivity, equation (4) is transformed to:

$$\frac{1}{\alpha} \frac{\partial T}{\partial t} - \nabla^2 T = \frac{f(r, t)}{\lambda} \quad (5)$$

This equation must be solved under certain boundary conditions. The body is defined as semi-infinite, i.e. limited by one plane $z = 0$. The heat source (electron beam) moves at a velocity v . The source is divided into two parts - surface and volume (Figure 1). The energy is distributed between the two parts in k_s/k_v ratio: $Q = k_s * Q_s + k_v * Q_v$. We take the ratio $k_s/k_v = 10/90$.

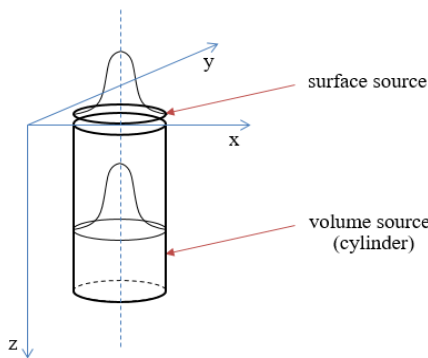


Figure 1. Scheme of the heat source.

The solution of equation (5) for a surface source in case of laser hardening by Green's functions is presented in [5]. A good agreement between the finite elements method (FEM) results and the analytical results obtained with Green's functions has been found.

The temperature distribution of a moving source is given as:

$$T_S(x, y, z, t) = \int_0^t \int_{-\pi}^{\pi} \int_0^{\infty} \frac{2\alpha}{\lambda} \frac{f_S(\xi, \eta, \tau)}{(4\pi\alpha(t-\tau))^{3/2}} \exp\left(-\frac{r^2 + z^2}{4\alpha(t-\tau)}\right) r dr d\theta d\tau \quad (6)$$

where

$$f_S(\xi, \eta, \tau) = \frac{3Q}{\pi r_0^2} \exp\left(-3 \frac{(\xi - v\tau)^2 + \eta^2}{r_0^2}\right) \quad (7)$$

is the intensity distribution for a moving source along a straight line with beam radius r_0 , in which the beam intensity falls to 5% of the maximum intensity, and with longitudinal beam velocity v , while x, y, z are the coordinates of the point of the calculated temperature, t is the time of the calculated temperature, $\xi = x - r \cos \theta$ and $\eta = y - r \sin \theta$, where r and θ are the polar coordinates of the points of the integration and Q is the transferred power.

The volume source beam distribution $f_V(\xi, \eta, \zeta, \tau)$ could have different forms depending on the type of the beam moving and the chosen shape of the source.

In the case of welding along a straight line, the shape of the heat source function could be chosen to be a cylinder with a base radius r_0 and height h with Gaussian distribution at any plane ζ and moving along a straight line. Then equation (6) is transformed to:

$$T_V(x, y, z, t) = \int_0^t \int_0^h \int_{-\pi}^{\pi} \int_0^{\infty} \frac{\alpha}{\lambda} \frac{f_V(\xi, \eta, \tau)}{(4\pi\alpha(t-\tau))^{3/2}} \left[\exp\left(-\frac{r^2 + (z-\zeta)^2}{4\alpha(t-\tau)}\right) + \exp\left(-\frac{r^2 + (z+\zeta)^2}{4\alpha(t-\tau)}\right) \right] r dr d\theta d\zeta d\tau \quad (8)$$

The intensity distribution of the cylinder heat source is defined as:

$$f_V(\xi, \eta, \tau) = \frac{3Q}{\pi r_0^2 h} \exp\left(-3 \frac{(\xi - v\tau)^2 + \eta^2}{r_0^2}\right) \quad (9)$$

The different influence of both the surface and the volume sources during the process of welding could be expressed as:

$$T(x, y, z, t) = k_v T_V(x, y, z, t) + k_s T_S(x, y, z, t) \quad (10)$$

EXPERIMENT

The investigated samples were made of constructive low alloy chrome-nickel steel 12XH3A with the chemical composition shown in Table 1. The thermophysical parameters of this steel are shown in Table 2.

Table 1. Chemical composition of steel 12XH3A.

Element	C	Si	Cr	Mn	Ni	P	S	Fe
wt, %	0.11	0.27	1.35	0.6	3.25	≤ 0.025	≤ 0.025	~ 95

Table 2. Thermophysical parameters of steel 12XH3A.

λ , W/(mm.K)	ρ , kg/m ³	C, J/(kg.K)	α , mm ² /s
0.0270	7680	540	6.510

Table 3. Technological parameters of the EBW process.

Specimen	Accelerating voltage	Beam current	Welding speed
No 1 – gear wheel	$U = 60$ kV	$I=50$ mA	$V=1.5$ cm/s
No 2 – plates	$U = 60$ kV	$I=50$ mA	$V=0.5$ cm/s
No 3 – plates	$U = 60$ kV	$I=50$ mA	$V=2$ cm/s

The samples were a real gear wheel and two specimens from identical plates welded with different welding speeds. Electron beam welding was carried out on the ESW300/15-60 welding units, manufactured by Leybold-Heraeus. The technological parameters of the EBW process are shown in Table 3. The measurement of residual stresses was performed on an FSD diffractometer at JINR - Dubna, Russian Federation [6-8]. The diffractometer was located on channel 11a of the IBP-2 impulse reactor. During the experiment a small volume of the sample was dedicated to being scanned with a neutron impulse flow. The sample was placed in front of a 90 ° detector. By moving the specimen, the diffraction spectrum was obtained at different sample points. The scanning was carried out on a horizontal axis perpendicular to the weld seam. The measured spectrum was analysed according to the Rietveld method. After the analysis, it was possible to determine the peaks in the spectra for deformed and undeformed material. The displacement of the peak position gives information about the deformation. Stresses were calculated under Hooke’s law at a known Young’s module value.

The microstructure of the welded specimens was investigated by scanning electron microscopy (SEM) on an EVO MA10 Carl Zeiss instrument. In particular, backscattering electrons were employed. The accelerated voltage was 20 kV.

RESULTS AND DISCUSSION

Figures 2 and 3 show the components of the stress tensor on each coordinate axis for the samples of the plates, and Figure 4 – the radial and axial components of the stress tensor for the gear wheel.

Alternating tensile and compressive stresses are observed. Stress values range from -150MPa to 800 MPa. The maximal levels of stress vary from 300 MPa to 800 MPa depending on the welding speed. Higher stresses are obtained at lower welding speeds. This is due to the greater linear energy ($Q_{lin.} = Q / v$) which is imported into the sample. A larger welding pool and higher temperature gradients are obtained. The temperature field is of great significance for the properties of the formed welding seam. The cooling speed is an important parameter on which the structure of the crystallized material depends. Therefore, we studied the temperature distribution using a theoretical model.

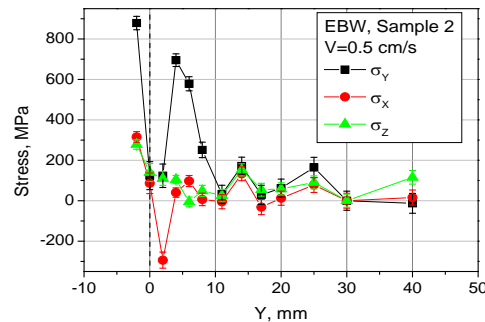


Figure 2. The stress distribution in specimen No 2 – EBW plates with welding speed $V=0.5$ cm/s.

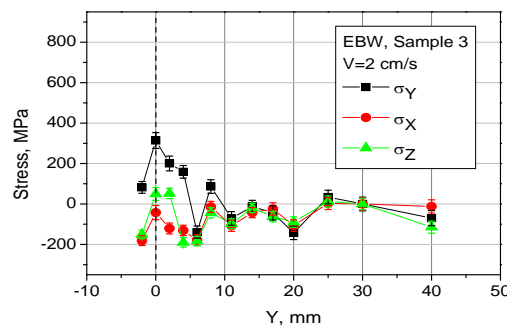


Figure 3. The stress distribution in specimen No 3 – EBW plates with welding speed $V=2$ cm/s.

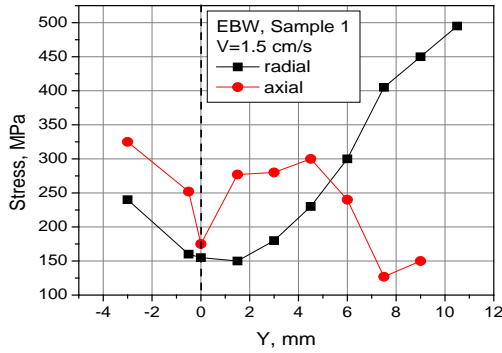


Figure 4. The stress distribution in specimen No 1 – EBW gear wheel with welding speed $V=1.5$ cm/s.

Using the above-mentioned equations (6-10) and numerical integration performed using the program Mathematica, the temperature distribution for the welding samples was calculated. In Figure 5 are shown the temperature cycles along the seam X for points on the surface of sample No3. Calculations are provided for two different Y- distances from the seam. In order to validate the model, analogous calculations were made using the analytical solution [9, 10]. A source model composed of a moving point source on the surface (10% of the power) and a moving linear source in a thin plate (90% of the power) was used. The results presented in Figure 5 show a good match between the temperature cycles calculated by the two models.

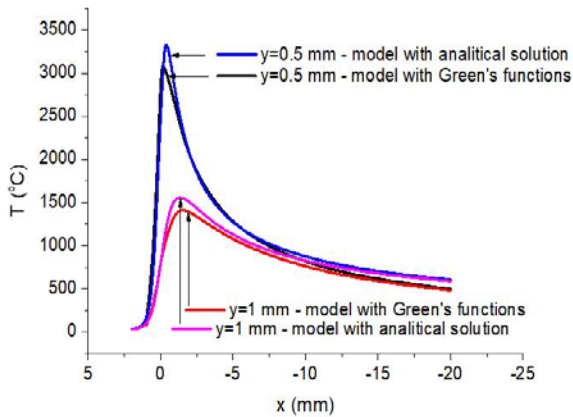


Figure 5. Temperature cycles for an electron beam welded specimen of 12XH3A steel plates with $Q=3$ kW and $V=2$ cm/s, determined by two different models

From the calculated temperatures a simulation of the melt zone of the welding seam and of the HAZ for specimen No. 3 was made. A good coincidence between the experimental and the theoretical form can be observed (Figure 6).

In Figure 7 is shown a part of the cross-sectional view from figure 6 made using SEM at $\frac{3}{4}$ of the depth of the welding seam.

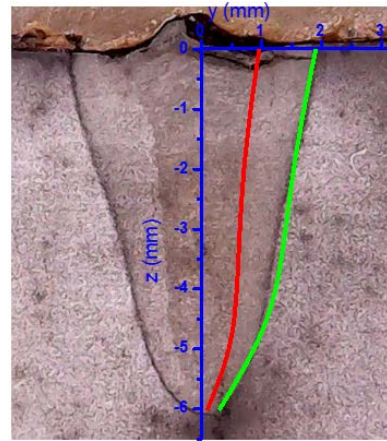


Figure 6. The macrograph of the cross-section of specimen No3 overlaid with the theoretically calculated form of the welding seam and the HAZ (on the right side of the picture).

The difference in the structures of the base metal, the HAZ and the molten zone (left to right of the picture) is clearly visible. By approaching the centre of the seam, the structure becomes finer. Considering the cooling speed, the structure of the material in the HAZ is a martensite. The weight Δy of the HAZ at this depth is approximately 500 μm .

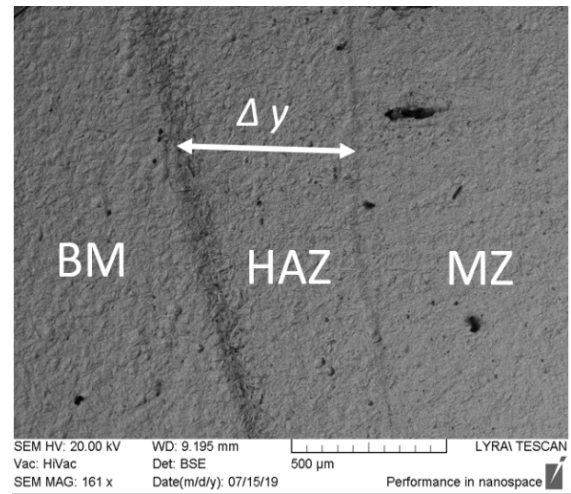


Figure 7. The SEM image of the cross-section of specimen No3 containing parts of base metal (BM), heat affected zone (HAZ) and melted zone (MZ) SEM at $\frac{3}{4}$ of the depth of the welding seam.

CONCLUSION

The residual stresses in EBW of gear wheel and of plates made from the same low-alloy steel 12XH3A were measured by neutron diffraction. The measured levels of residual stresses are quite low. The maximal stress level is varying in the range from 300 MPa to 800 MPa for welded plates and it is up to 500 MPa for the gear wheel. It was established that residual stresses in the welding joint and in the HAZ depend strongly on the welding speed. The temperature fields were

calculated using a model of moving source containing surface and volume cylindrical parts. The calculation was based on the application of Green`s functions. The theoretical temperatures show a good agreement with the experiment. The temperature distribution depends on the technological parameters of the welding process. The observed martensitic structure corresponds to the cooling speed found by the temperature cycles.

Acknowledgements: *The authors would like to thank the Bulgarian Nuclear Regulatory Agency for providing financial support and the Bulgarian National Scientific Fund (Contract No. DN 07/26).*

REFERENCES

1. ASM Handbook, Vol. 1, Properties and Selection: Irons, Steels, and High Performance Alloys, ASM International, 1990.
2. H. Schultz, Electron Beam Welding, Woodhead Publishing, 1994.
3. N. S. Rossini, M. Dassitsi, K. Y. Benyounis, A. G. Olabi, *Mater. Design*, **35**, 572 (2012).
4. M. T. Hutchings, P. J. Withers, T. M. Holden, T. Lorentzen, Introduction to the Characterization of Residual Stress by Neutron Diffraction, CRC Press, 2005.
5. G. Farrahi, M. Sistaninia, *Int. J. Eng: Transactions A: Basics*, **22**, 169 (2009).
6. G. D. Bokuchava, V. L. Aksenov, A. M. Balagurov, E. S. Kuzmin, V. V. Zhuravlev, A. P. Bulkin, V. A. Kudryashev, V. A. Trounov, *Appl. Phys. A- Mater.*, **74** (Suppl. 1), 86 (2002).
7. G. D. Bokuchava, A. M. Balagurov, V. V. Sumin, I. V. Papushkin, *J. Surf. Invest. X-ray*, **4**, 879 (2010).
8. G. Bokuchava, *Crystals*, **8**, 318, (2018).
9. D. Rosenthal, *Weld. J.*, **20** (5), 220 (1941).
10. V. Mihailov, V. Karhin, P. Petrov, Fundamentals of welding (in English), Polytechnic University Publishing, St. Petersburg, 2016.